Supporting information for manuscript

Voltage Scanning to Calibrate Multi-Reagent Chemical Ionization Mass Spectrometers (MR-CIMS): From Signal to Sensitivity

Table of Contents:

Figure S10. RH dependence of Cl^- and $BrCl_2^-$ in bromide channel. The dashed line indicates the water ratio in the bromide channel under routine measurements and during voltage scanning. Errors represent the standard deviation of data obtained at the same water ratio.

Section S1. The set of voltage bias and voltage settings during voltage scanning.

The Vocus AIM (adduct ionization mechanism) IMR (ion-molecule reactor) is grounded, and its electric potential is thus fixed. We do not want the adjustments of voltages to influence the transmission before BSQ (big segmented quadrupole). To avoid this, a voltage bias can be set between IMR and SQ (short quadrupole) to ensure that the injection of ions into SQ is purely driven by gas expansion. A voltage bias of 4 V is an empirically determined value that can achieve this goal. It ensures the difference in the binding energies of adducts can be observed during the voltage scanning. There is also a drawback to doing this. By setting such a voltage bias, certain ions are rejected and thus the signals detected by the detector will decrease. In our instruments, the total ion counts (TIC) are reduced by half (**Figure S1**). Therefore, this increases the threshold of signals applicable to voltage scanning and is not recommended to set in routine use. During the voltage bias setting and voltage scanning, the water regulation is stopped in order to avoid the variations of relative humidity (RH) in IMR.

Section S2. Kernel density estimation (KDE) on the distributions of dV_{50}

Kernel density estimation (KDE) has been widely used on estimating probability density functions.[1] It is a well-known method and programmed efficiently in Seaborn package. We introduced it to ensure the completeness of the manuscript. The function of KDE is:

$$\hat{f}(x) = \frac{1}{nh}\sum_{i=1}^{n} K\left(\frac{x-x_i}{h}\right) \quad \text{(Eq.2.1)}$$

where n is the number of data point and is the number of compounds in our case, h is the bandwidth, K is the Gaussian distribution function, and x_i in our case is the dV_{50} of compound i. The bandwidth h is estimated using Scott's Rule,[2] whose function is:

$$h = 1.06 \cdot \sigma \cdot n^{-1/(d+4)} \quad \text{(Eq.2.2)}$$

where d is the number of dimensions and is 1 here. We applied a factor of 0.7 on bandwidth to show more details of probability density functions at the expense of some smoothness.

The exact implementation can be examined in the source code of the kde.py in the Seaborn library (https://github.com/mwaskom/seaborn/blob/master/seaborn/external/kde.py, last access: August 6, 2025). We conducted KDE on compounds with different oxygen levels separately.

Section S3. Calculation methods of noise and signal-to-noise ratio (SNR)

The noise of a certain analyte, i, at time point, j, is calculated using Eq.3.1,

$$N_{ij} = \sigma_{ij} + \sigma_{noise,j} \quad \text{(Eq.3.1)}$$

The SNR of a certain analyte, i, at time point, j, is calculated using Eq.3.2,

$$SNR_{ij} = \frac{I_{ij}}{N_{ij}} \quad \text{(Eq.3.2)}$$

I_{ij} is the signal intensity normalized with the reagent ion intensities (ncps). Assuming that it follows Poisson distribution, σ_{ij} is the analytical uncertainty from counting statistics in the mass spectrum and is calculated using $\sigma_{ij} = a\sqrt{I_{ij}/\,t_s}$. a is an empirically determined factor incorporating any unaccounted contributions to the uncertainty and here we follow the value 1.28 utilized in the previous studies.[3] t_s is the integration time in seconds. $\sigma_{noise,j}$ is the standard deviation of blank masses spectrum (m/z > 650 Th) and is calculated to be in the range of 1.54 – 1.90 ncps and 1.26 – 1.61 ncps for bromide-channel and iodide channel at an integration time of 1 s, respectively, throughout the campaign.

Table S1. Voltage settings of the MR-CIMS during voltage scanning. Only the adjusted voltages are listed below. All values are given in volts.

	Negative channels				Positive channels			
	Reactor back	Quad DC (bias)	Quad linac	Skimmer	Reactor back	Quad DC (bias)	Quad linac	Skimmer
Before scanning	0	0	0	0	0	0	0	-1
Step 1	-4	0	0	0	4	0	0	-1
Step 2	-4	-1	-1	-1	4	1	1	0
Step 3	-4	-2	-2	-2	4	2	2	1
Step 4	-4	-3	-3	-3	4	3	3	2
Step 5	-4	-4	-4	-4	4	4	4	3
Step 6	-4	-5	-5	-5	4	5	5	4
Step 7	-4	-6	-6	-6	4	6	6	5
Step 8	-4	-7	-7	-7	4	7	7	6
Step 9	-4	-8	-8	-8	4	8	8	7
Step 10	-4	-9	-9	-9	4	9	9	8
Step 11	-4	-10	-10	-10	4	10	10	9
Step 12	-4	-11	-11	-11	4	11	11	10
Step 13	-4	-12	-12	-12	4	12	12	11
Step 14	-4	-13	-13	-13	4	13	13	12
Step 15	-4	-14	-14	-14	4	14	14	13
Step 16	-4	-15	-15	-15	4	15	15	14
Step 17	-4	-16	-16	-16	4	16	16	15

Table S2. Calibrants, their calibration methods, and sensitivities in MR-CIMS. The sensitivities were calibrated at a water ratio of 0.6 in Iodide-channel, where the uncertainty corresponds to the 95% confidence interval obtained from the linear fit.

	Calibration methods	Sensitivity in Bromide-channel (ncps/pptv)	Sensitivity in Iodide-channel (ncps/pptv)
Chlorine (Cl_2)	Standard cylinder	11.33 ± 0.37	3.27 ± 0.40
Formic acid (CH_2O_2)	Permeation tube	6.80 ± 0.36	2.60 ± 0.18
Nitric acid (HNO_3)	Permeation tube	14.08 ± 1.41	9.27 ± 1.65
Acetic acid ($C_2H_4O_2$)	LCS	0.46 ± 0.21	0.03 ± 0.02
Butanoic acid ($C_4H_8O_2$)	LCS	0.53 ± 0.03	0.02 ± 0.002
Propylene glycol ($C_3H_8O_2$)	LCS	0.28 ± 0.01	0.03 ± 0.01
Pyruvic acid ($C_3H_4O_3$)	LCS	3.47 ± 0.22	0.11 ± 0.03
Ethylene glycol ($C_2H_6O_2$)	LCS	0.23 ± 0.02	0.02 ± 0.01
Glyoxylic acid ($C_2H_2O_3$)	LCS	8.98 ± 0.58	3.56 ± 0.78
Glycolic acid ($C_2H_4O_3$)	LCS	10.34 ± 0.48	4.67 ± 0.33
Salicylic acid ($C_7H_6O_3$)	LCS	9.08 ± 0.63	2.13 ± 0.28
2-nitrophenol ($C_6H_5NO_3$)	LCS	Adduct undetected	Adduct undetected
3-nitrophenol ($C_6H_5NO_3$)	LCS	13.51 ± 0.53	9.61 ± 0.39
4-nitrophenol ($C_6H_5NO_3$)	LCS	12.62 ± 0.38	9.61 ± 0.28

Figure S1. (a) Time series of IMR pressure, SQ pressure, and IMR temperature during a representative experiment. A background check was performed every 30 min by introducing UHP N_2 into the IMR, which caused spikes in the pressure. The pressures returned to their setpoints within approximately 4 s. Histograms of (b) IMR pressure, (c) SQ pressure, and (d) IMR temperature values during this representative experiment.

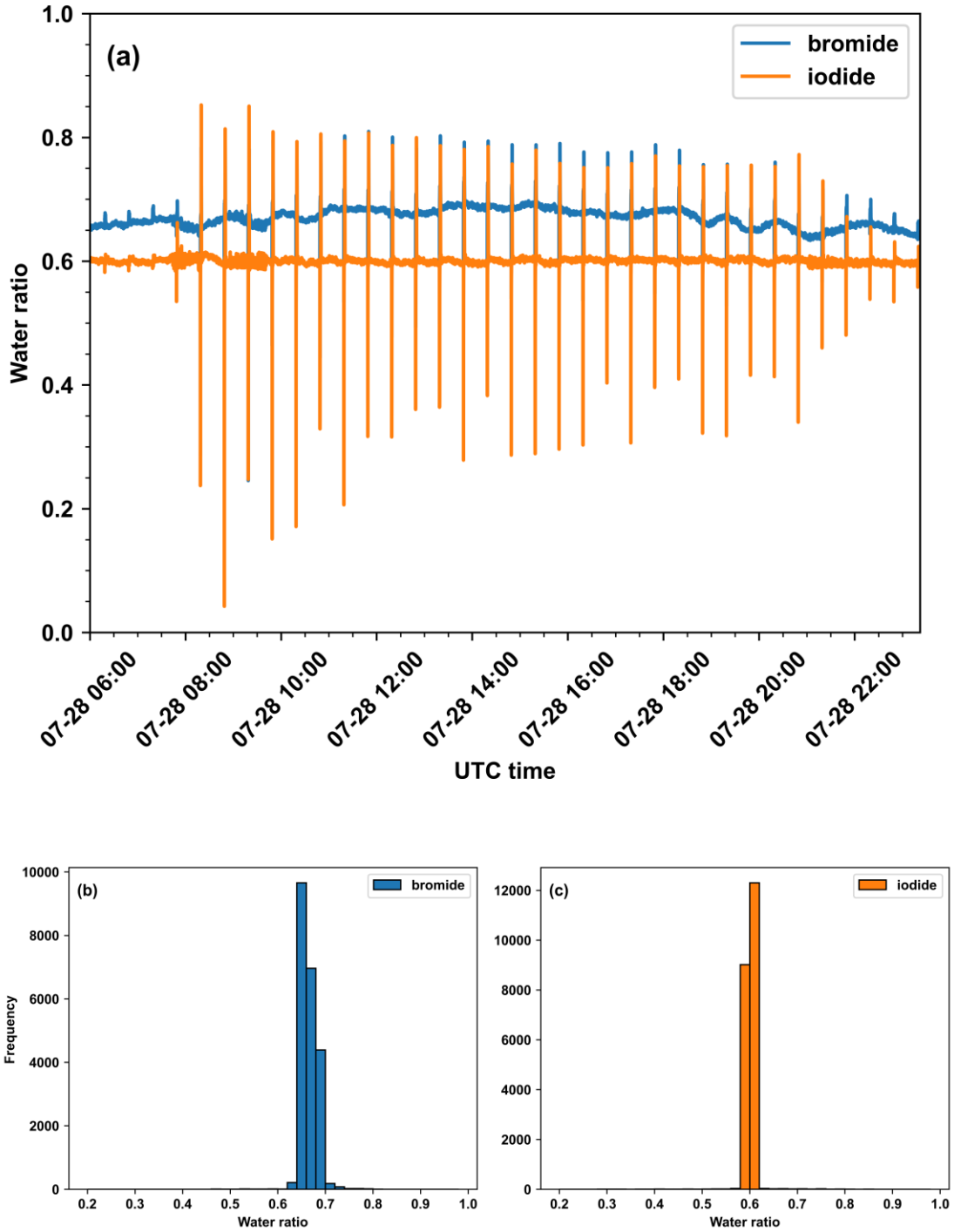

Figure S2. (a) Time series of water ratio in bromide and iodide channel during a representative experiment. A background check was performed every 30 min by introducing UHP N_2 into the IMR, which caused spikes in the water ratio. The pressures returned to their setpoints within approximately 4 s. Histograms of water ratio in (b) bromide channel and (c) iodide channel during this representative experiment, using a bin width of 0.2.

(a)

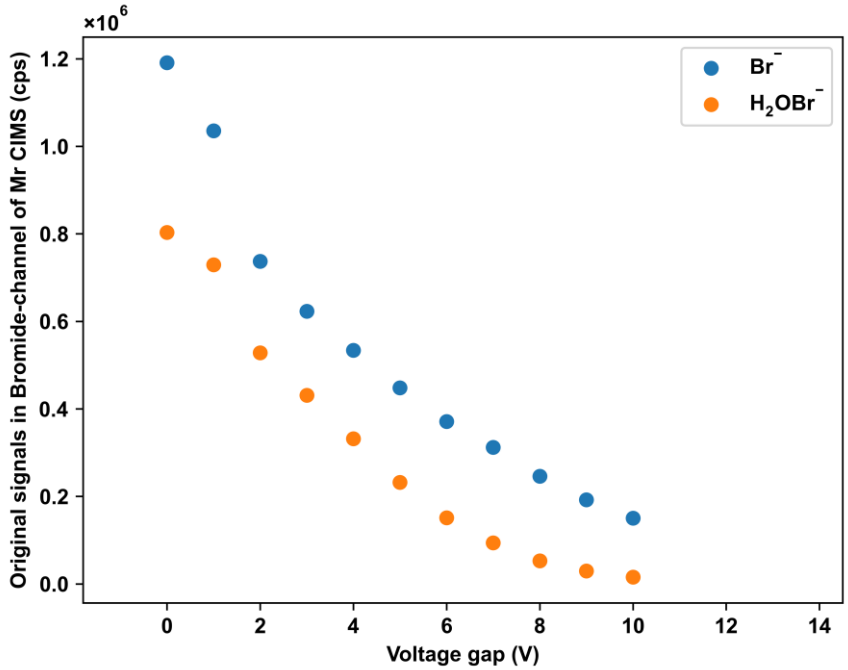

(b)

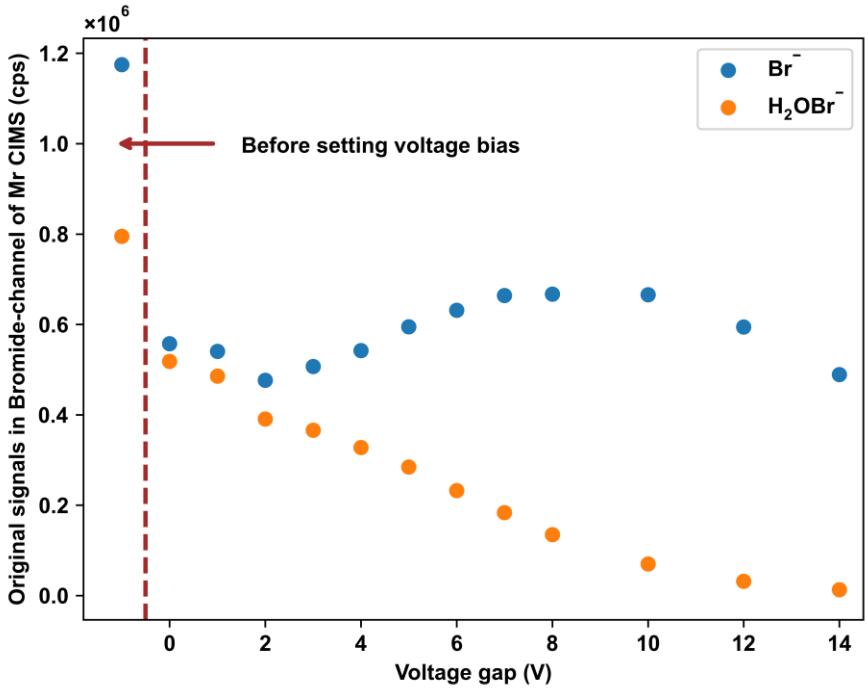

Figure S3. Signal variations of Br^- and H_2OBr^- (a) without a voltage bias and (b) with a voltage bias during the voltage scanning.

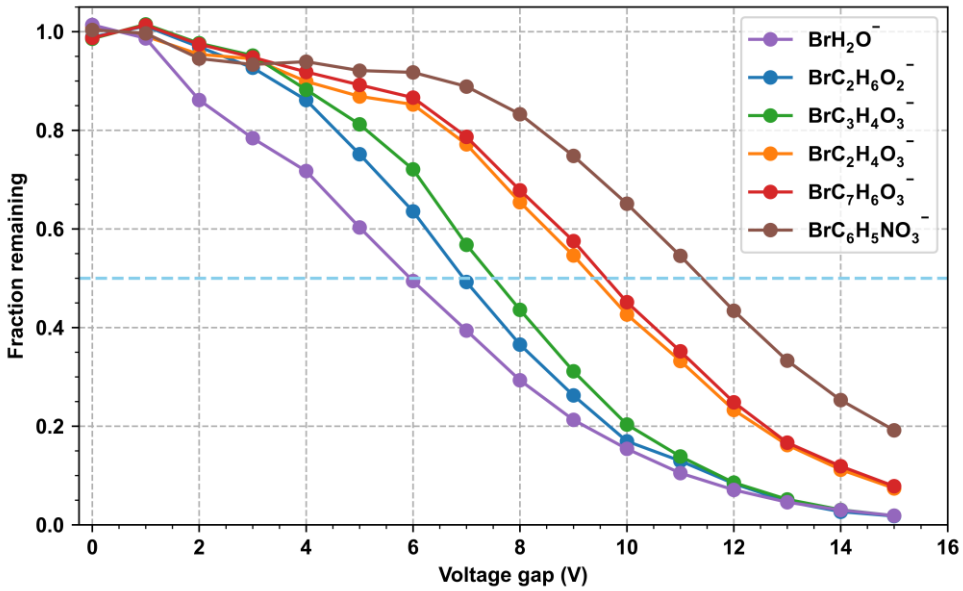

Figure S4. Representative dissociations of ion–molecule adducts in the bromide channel. Signals of adducts have been normalized to the sum of reagent ions and hydrated reagent ions and to the maximum at the start of the voltage scanning. The blue dashed horizontal line indicates the voltage gap where the signals of adducts decreased by a factor of two, i.e., dV_{50}.

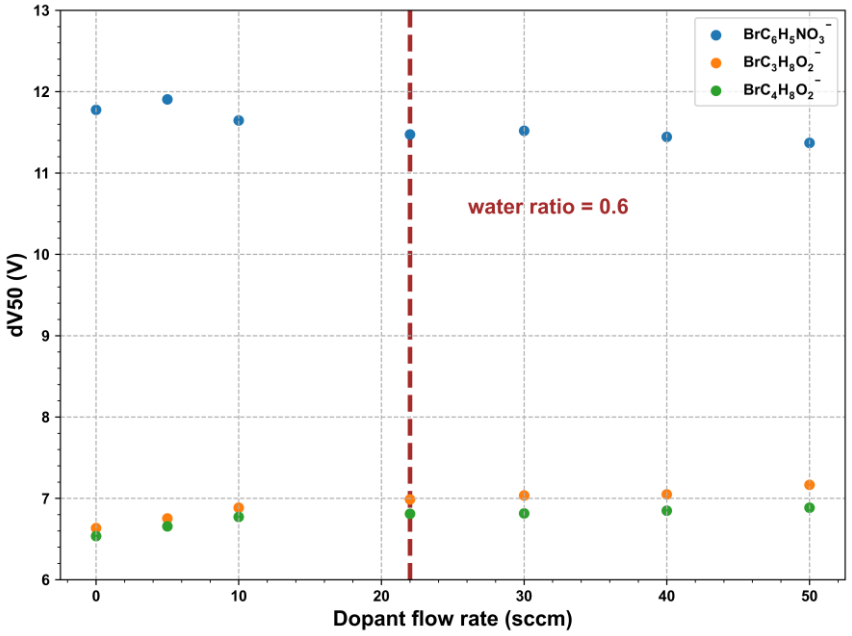

Figure S5. The influences of dopant flow on dV_{50} of 3-ntrophenol, propylene glycol, and butyric acid in bromide channel. The dashed line represents the conditions with a water ratio of 0.6 in the iodide channel, which corresponds to the routine measurement setting.

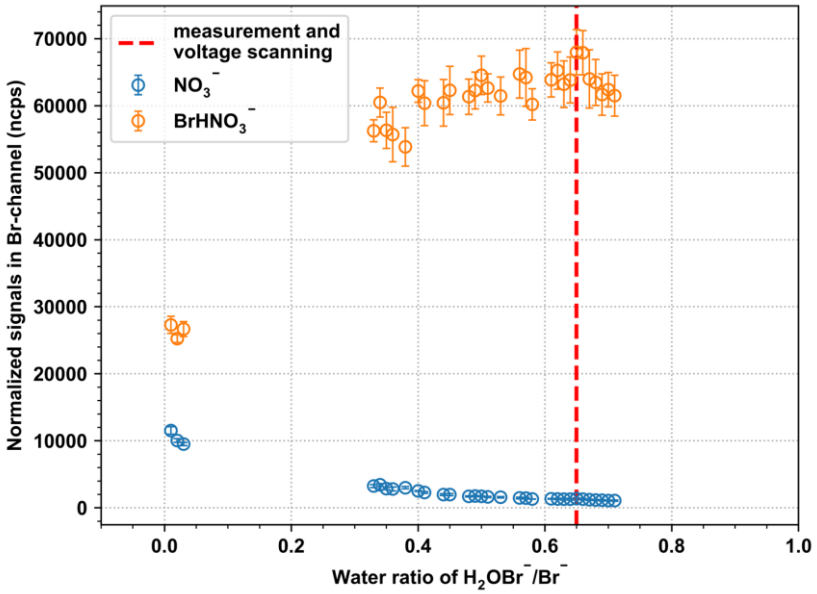

Figure S6. RH dependence of NO_3^- and $BrHNO_3^-$ in bromide channel. The dashed line indicates the water ratio in the bromide channel under routine measurements and during voltage scanning. Errors represent the standard deviation of data points obtained at the same water ratio.

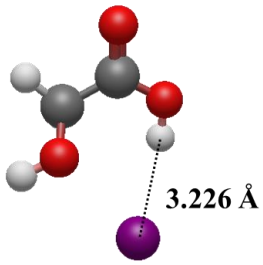

Figure S7. Geometries of clusters between I^- and glycolic acid. Color coding: oxygen, red; carbon, gray; hydrogen, white; iodide, purple. Hydrogen bond lengths were labeled in the plot.

(a)

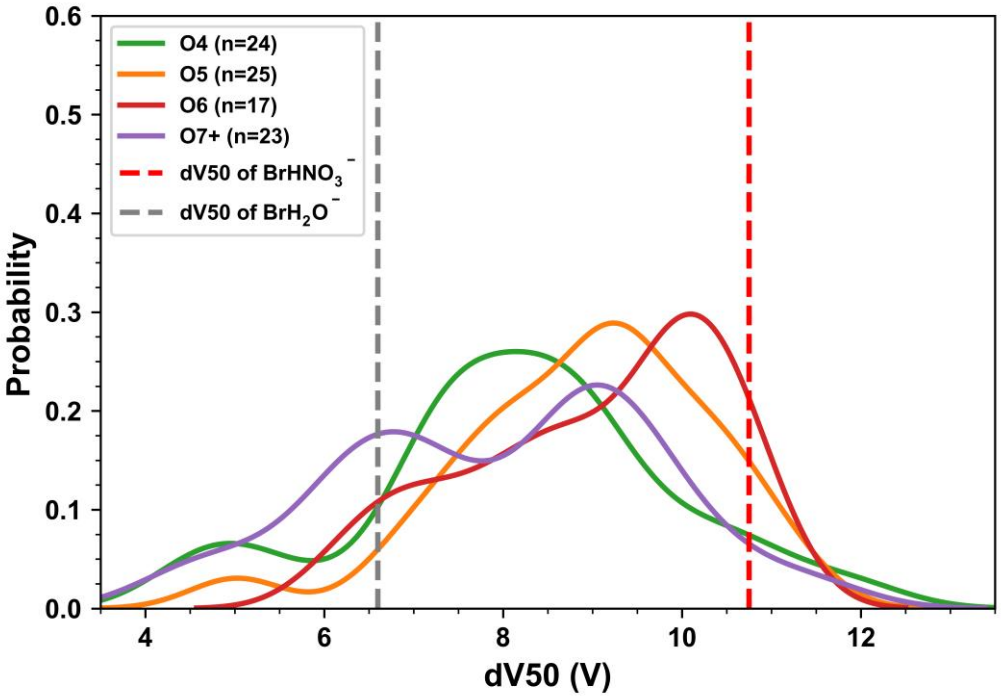

(b)

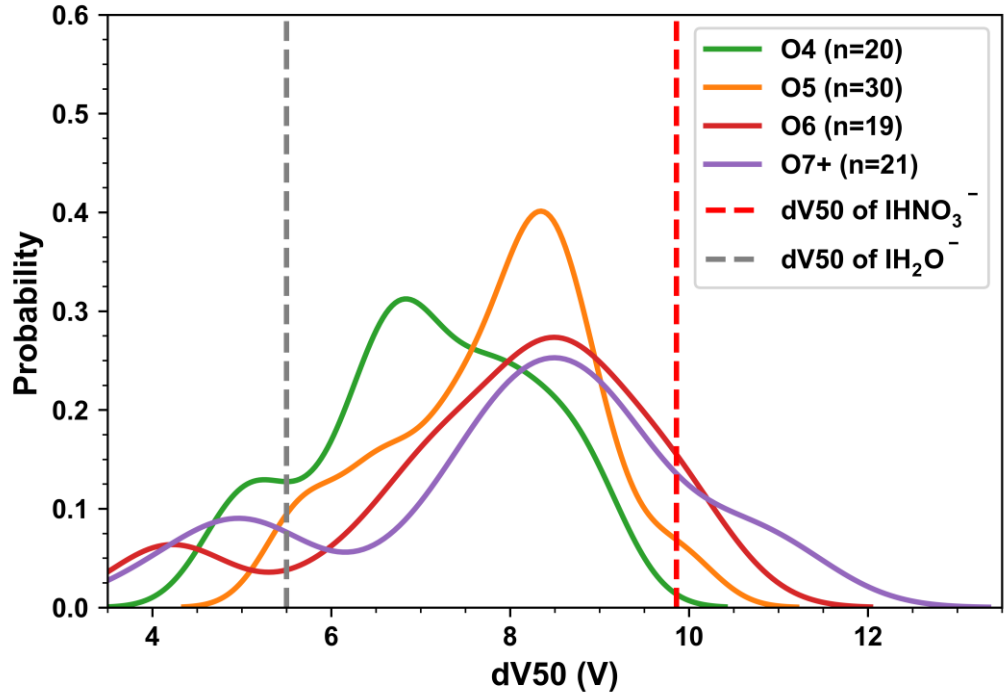

Figure S8. Distributions density of dV_{50} for compounds $C_xH_yNO_z$ ($z \geq 4$) detected in the (a) bromide channel and (b) iodide channel of MR-CIMS. dV_{50} of water and nitric acid in each channel are shown for comparison. Compounds with oxygen content outside this range were not plotted for clarity. The number of compounds in each category are shown in the label.

(a)

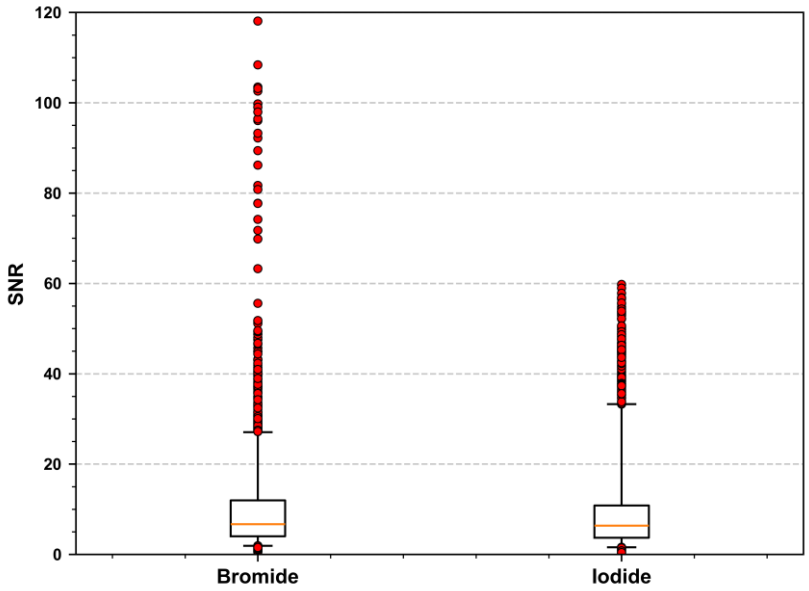

(b)

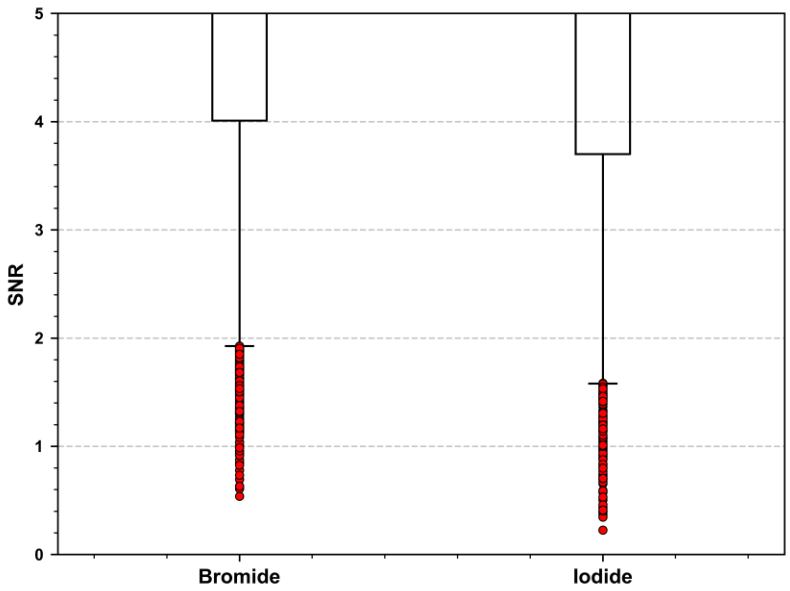

Figure S9. (a) Distributions of SNRs for adducts in bromide channel and iodide channel with successful voltage scanning. The whiskers represent the 5th and 95th percentiles, while the box spans the interquartile range (25th to 75th percentile), with the red line denoting the median. Red points stand for the outliers. (b) A magnified view of the distribution.

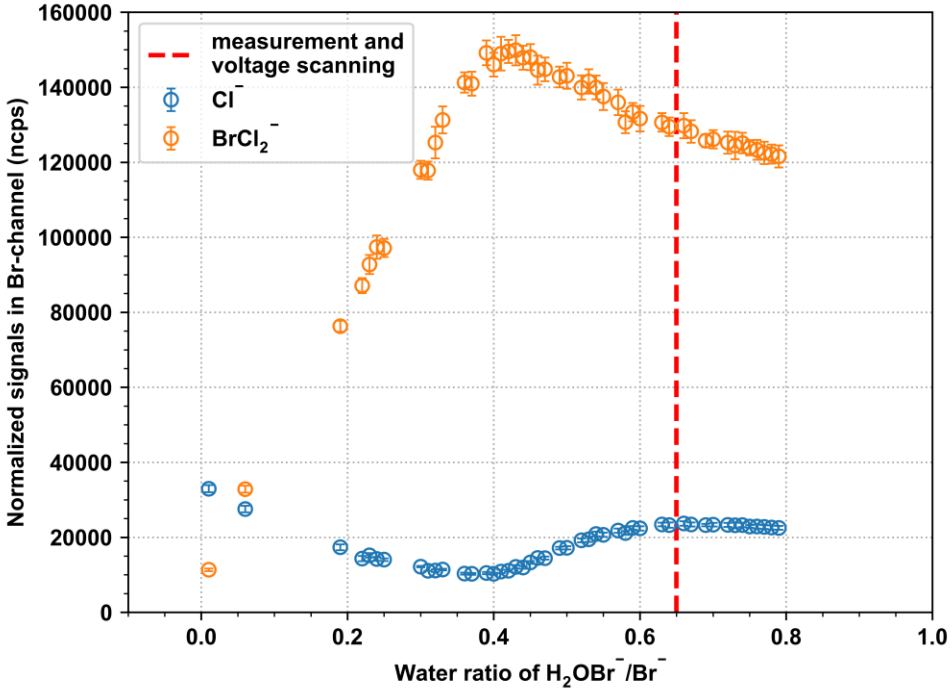

Figure S10. RH dependence of Cl^- and $BrCl_2^-$ in bromide channel. The dashed line indicates the water ratio in the bromide channel under routine measurements and during voltage scanning. Errors represent the standard deviation of data obtained at the same water ratio.

References

(1) Silverman, B. W. *Density Estimation for Statistics and Data Analysis*; Routledge, 2018. https://doi.org/10.1201/9781315140919.

(2) Scott, D. W. On Optimal and Data-Based Histograms. *Biometrika* **1979**, *66* (3), 605–610. https://doi.org/10.1093/biomet/66.3.605.

(3) Yan, C.; Nie, W.; Aïjälä, M.; Rissanen, M. P.; Canagaratna, M. R.; Massoli, P.; Junninen, H.; Jokinen, T.; Sarnela, N.; Häme, S. A. K.; Schobesberger, S.; Canonaco, F.; Yao, L.; Prévôt, A. S. H.; Petäjä, T.; Kulmala, M.; Sipilä, M.; Worsnop, D. R.; Ehn, M. Source Characterization of Highly Oxidized Multifunctional Compounds in a Boreal Forest Environment Using Positive Matrix Factorization. *Atmos. Chem. Phys.* **2016**, *16* (19), 12715–12731. https://doi.org/10.5194/acp-16-12715-2016.